
Bond Graph Modelling and Simulation of Pneumatic Soft Actuator

Garima Bhandari · Pushparaj Mani Pathak ·
Jung-Min Yang

the date of receipt and acceptance should be inserted later

Abstract This paper presents the design and dynamic modelling of a soft pneumatic actuator that can be used to mimic snake or worm-like locomotion. The bond graph technique is used to derive the dynamics of the actuator. To validate the accuracy of the derived dynamic model, we conduct numerical simulations using 20-sim[®] software. Experimental results demonstrate that the soft actuator achieves bi-directional bending and linear displacement, which is essential for mimicking snake or worm-like locomotion.

Keywords Bond graph · Control · Dynamics · Snake robots · Soft robots.

1 Introduction

In nature many limbless reptiles with slender bodies use their body's flexibility and frictional properties to move around and overcome obstacles in environment. This has inspired new field of soft robots which mimic the motions of natural creatures like a snake, elephant trunk, etc. The rigid robots will require an infinite number of joints to realize the flexibility to mimic the behavior of snake locomotion, which is not an energy-efficient solution. Whereas soft robots have an infinite passive degree of freedom (DoFs), enabling them to be passively deformed when interacting with environments under simple actuation. Another advantage of soft robots over conventional rigid robots is safe interaction with humans and adaptability to complex and uncertain environment at low-cost (Laschi et al, 2016).

Several soft robots perform various movements as bending, rotation, extending/contracting, and twisting using multiple techniques and materials, including shape memory alloys, shape morphing polymers, dielectric elastomers, tendon drive, piezoelectric actuation, and fluid power (Blumenschein et al, 2018; Elango and Faudzi, 2015; Elango et al, 2020; Zhang et al, 2019). Amongst these, pneumatically-driven are found most advantageous because of their large deformation/force, good power-to-weight ratio, and low manufacturing cost (Mohd Nordin et al, 2013). They have gained popularity as a fiber-reinforced soft bending actuator (FRSBA) (Deimel and Brock, 2013), but the

Supported by organization DST, India and NRF, South Korea.

Indian Institute of Technology Roorkee, Haridwar-24766, Uttarakhand, India · Kyungpook National University, 80, Daehak-ro, Buk-gu, Daegu, South Korea

E-mail: gsoharu@me.iitr.ac.in, pushparaj.pathak@me.iitr.ac.in

E-mail: jmyang@ee.knu.ac.kr

use of viscoelastic material makes soft robots a highly non-linear system. The non-linearity of the dynamics of the soft robots increases the complexity of control (Boyraz et al, 2018), due to which most control strategies are open-loop in the case of soft robots (Huang et al, 2019).

Few studies have attempted to implement close loop control by dynamically controlling the fluid pressure or mass inside the robot body (Deimel et al, 2016; Gerboni et al, 2017). Some have ignored dynamics completely and tried model-free control methods or training methods (Polygerinos et al, 2015; Wu et al, 2018). But ignoring dynamics does not guarantee accurate control performance. Further, few studies implemented theoretical kinematics and dynamics models for controller design. These studies included various approaches, including finite element method(FEM), constant curvature method, concentrated mass method, and Euler-Lagrange method (Falkenhahn et al, 2017; Marchese et al, 2016; Thor Morales et al, 2018). The dynamics provided by before mentioned methods are ambiguous, complex, and difficult to analyze, thus making controller design difficult. Further few studies implemented empirical methods such as Jacobian method (Li et al, 2018), visual servo control (Greer et al, 2017), neural network, sliding mode control and adaptive control (Hyatt et al, 2019; Skorina et al, 2017). These studies provide a simpler approach toward system modeling and controller design than the strategies involving more complex theoretical models. However, the nonlinear behaviors are not perfectly described, and the validities are limited to the specified experimental conditions (Chen et al, 2020).

The paper presents a simple soft actuator design based on has bi-directional bending and stretching/contracting capabilities due to which it can have snake or worm-like movements. The actuator can be used in various applications as a manipulator or mobile robot. Further, a dynamic model of the soft actuator has been derived from the bond graph modelling approach. The proposed modeling formalism can accommodate major dynamic parameters of the soft actuator and system non-linearities. The robot has been controlled using PD controller. The performance of the soft actuator modelling is validated through numerical simulations where the soft robot emulates bi-directional bending and extension/contraction as desired by the controller input.

The rest of this paper is structured as follows. Section 2 presents the design and modelling of a soft actuator in framework of bond graph technique. Section 3 presents detailed numerical simulation results to validate proposed dynamics with close-loop PD control implemented. Finally, Section 4 concludes the paper.

2 Dynamic Modelling

We will discuss the dynamics of the soft actuator in this section. To understand the dynamics it is important to understand the working and design of the soft actuator. The following sections explains in detail the design and bond graph modelling of the actuator.

2.1 Design of Soft Actuator

The design of the soft actuator is bellow-like. The soft actuator has packets made of elastic material joined together, as shown in Fig. 1.

The elastic packets inflate and deflate like balloons when air is supplied or removed from them. The two-way air pump can supply and remove air; the connection of air pump to soft actuator is as shown in Fig. 1. The bidirectional bending is emulated by alternating supplying and removing air from each side of the soft actuator. The actuator bends in the direction of the side from where the pump removes air.

The micro-controller controls the alternating air supply and removal of air for bidirectional bending. We can attach various sensors to the soft actuator to measure the pressure, extension, and bending angle and employ them to control the soft actuator. Fig. 2a-2b shows solid model and the

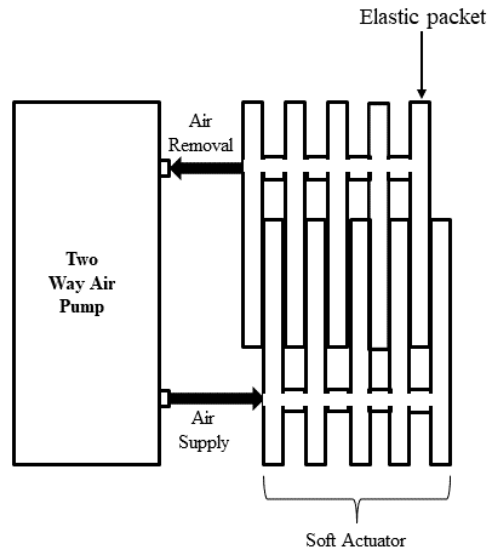


Fig. 1 Schematic representation of working concept.

pictorial representation of the working concept of the soft actuator. Now with a clear understanding of working and control of soft actuator, we will model the bond graph to derive the dynamics in the next section.

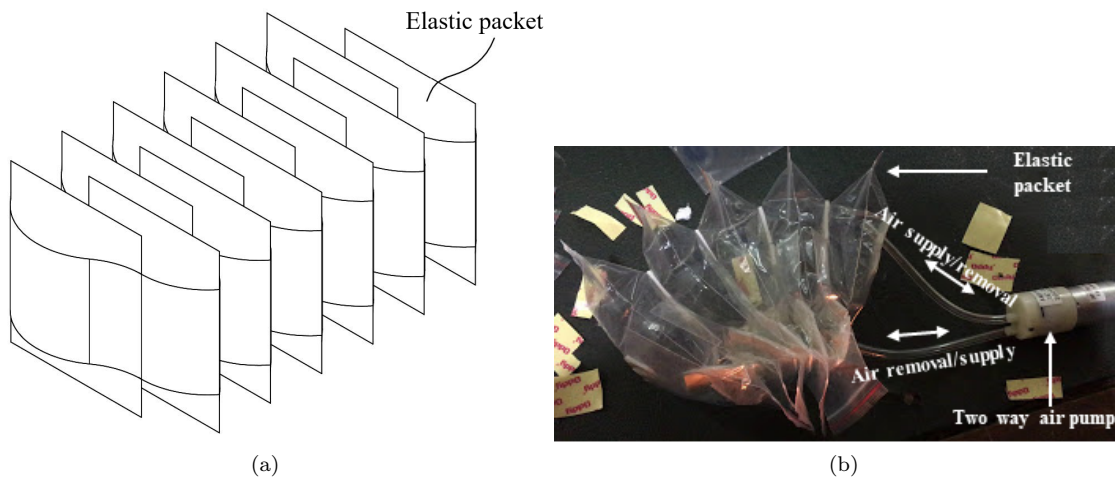


Fig. 2 Soft actuator's (a) solid model, and (b) pictorial representation of its working concept.

2.2 Bond Graph Modelling of Soft Actuator

The bond graph modelling technique reduces mathematical complexities related to highly non-linear system, such as soft actuator presented in this paper. Since our actuator design is bellow-like, so we model each elastic packet as a bellow. For the basic understanding of bond graph model, we explain Fig. 3. in detail.

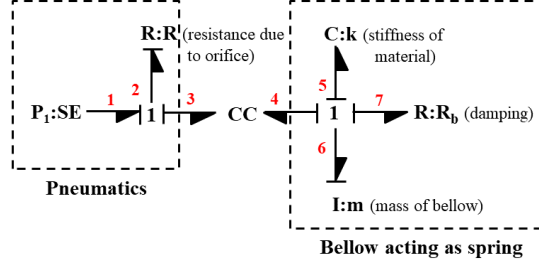


Fig. 3 Bond graph of the bellow.

The source of effort element (**SE**), is the pressure (P_1) supplied to the elastic packet from the air pump. The resistance element (**R**), is the resistance the pneumatic flow faces when it enters through the orifice in the elastic packet. We calculate value of resistance as:

$$R = \frac{\sqrt{P_1 - P_2}}{C_d D} \quad (1)$$

where, C_d , is the orifice coefficient of discharge, and D is diameter of orifice.

We have assumed extension and contraction of soft actuator synonymous with that of spring for the ease of modelling; with this assumption, we infer that the effort from the pneumatic domain is causing displacement in the mechanical part. We use C-field element (**CC**) in cases like these where the efforts and displacements are in a different domain but interrelated. Thus we have two capacitance values in this system, C_1 , due to change in volume of the elastic packet and C_2 , due to compressibility of air (Bolton, 1999). We can calculate their value as follows:

$$C_1 = \frac{A^2}{k} \quad (2)$$

$$C_2 = \frac{Ax}{\rho RT}$$

where A and k are the area and stiffness of elastic packet respectively, x is the extension in the elastic packet after air supply, ρ is the density of air, R is gas constant, and T is the temperature of air supplied.

The resistance element (**R**) represented as R_b is damping in elastic packet and inductance element (**I**), is its mass (m). The dynamic equations we get after bond graph modelling are:

$$R(C_1 + C_2) \frac{dP_2}{dt} + P_2 = P_1 \quad (3)$$

$$m\ddot{x} + R_b\dot{x} + kx = P_2A \quad (4)$$

where P_2 is the pneumatic pressure inside the elastic packet, which is given by effort in bond number 3 in Fig. 3.

The bond graph model of elastic packet is then used to make the both sides of the actuator as shown in Fig. 4. We have implemented half car model for bidirectional bending of the actuator.

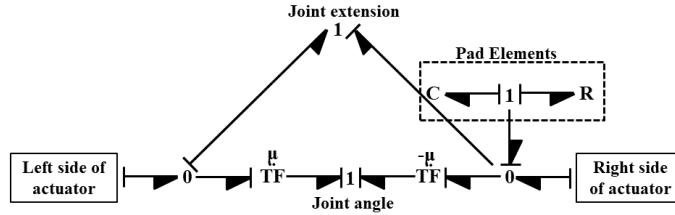


Fig. 4 Bond graph of the actuator.

Since we want to alternately supply and remove air from each side of actuator, the pressure P_1 is provides as:

Left side of actuator

$$P_1 = k_p(x_{Lref} - x_L) + k_d(\dot{x}_{Lref} - \dot{x}_L) \quad (5)$$

$$\text{where, } x_{Lref} = x \sin(\omega t)$$

Right side of actuator

$$P_1 = k_p(x_{Rref} - x_R) + k_d(\dot{x}_{Rref} - \dot{x}_R) \quad (6)$$

$$\text{where, } x_{Rref} = x \sin(\omega t + \pi)$$

k_p and k_d are proportional and derivative control gains, whereas x_L and x_R are actual extension or contraction of left and right side of the actuator.

From Eqs.5-6 we infer that we alternately supply air to the left side of the actuator and remove air from its right side, thus making it bend in both directions. We can also achieve simple extension and contraction by providing air supply as in Eq.5 on both sides of the actuator.

3 Numerical simulations

After creating bond graph model of actuator, we conduct numerical simulations to validate its accuracy in the framework of 20-sim® (ver. 4.7) (Controllab Products, 2018). Table 1 summarizes the system parameters of actuator used in the numerical experiment.

Figs. 5a and 5b shows results for bi-directional bending of actuator. We can see in, Fig. 5a, each side of actuator extends and contracts alternately according to x_{ref} for each side. Fig. 5b shows the result for bi-directional bending and rotation angle achieved. We can see there is no linear displacement in this case.

The extension and contraction of both sides of the actuator for linear displacement of the actuator are drawn in Fig. 5c. In this case, we can see both sides of the actuator are expanding and contracting simultaneously. Fig. 5d demonstrates that the actuator has only linear displacement when each side expands and contracts simultaneously.

Table 1 System parameters used in numerical experiment.

Parameter	Value	Parameter	Value
m	0.015 kg	x	0.3 m
R_b	0.4 kg/sec	ρ	1.225 kg/m ³
k	350 N/m	R	8.31451 J/K mol
C_d	0.8	T	300 K
D	0.008 m	k_p	40
A	0.0096 m ²	k_d	10
μ	2.5	ω	1 rad/sec

As explained in section. 2.2 controller output is pressure, P_1 , supplied to actuator (see Eqs. 5–6). Fig. 6 shows the results for rotation angle, linear displacement and torque generated by actuator for the controlled pressure supply.

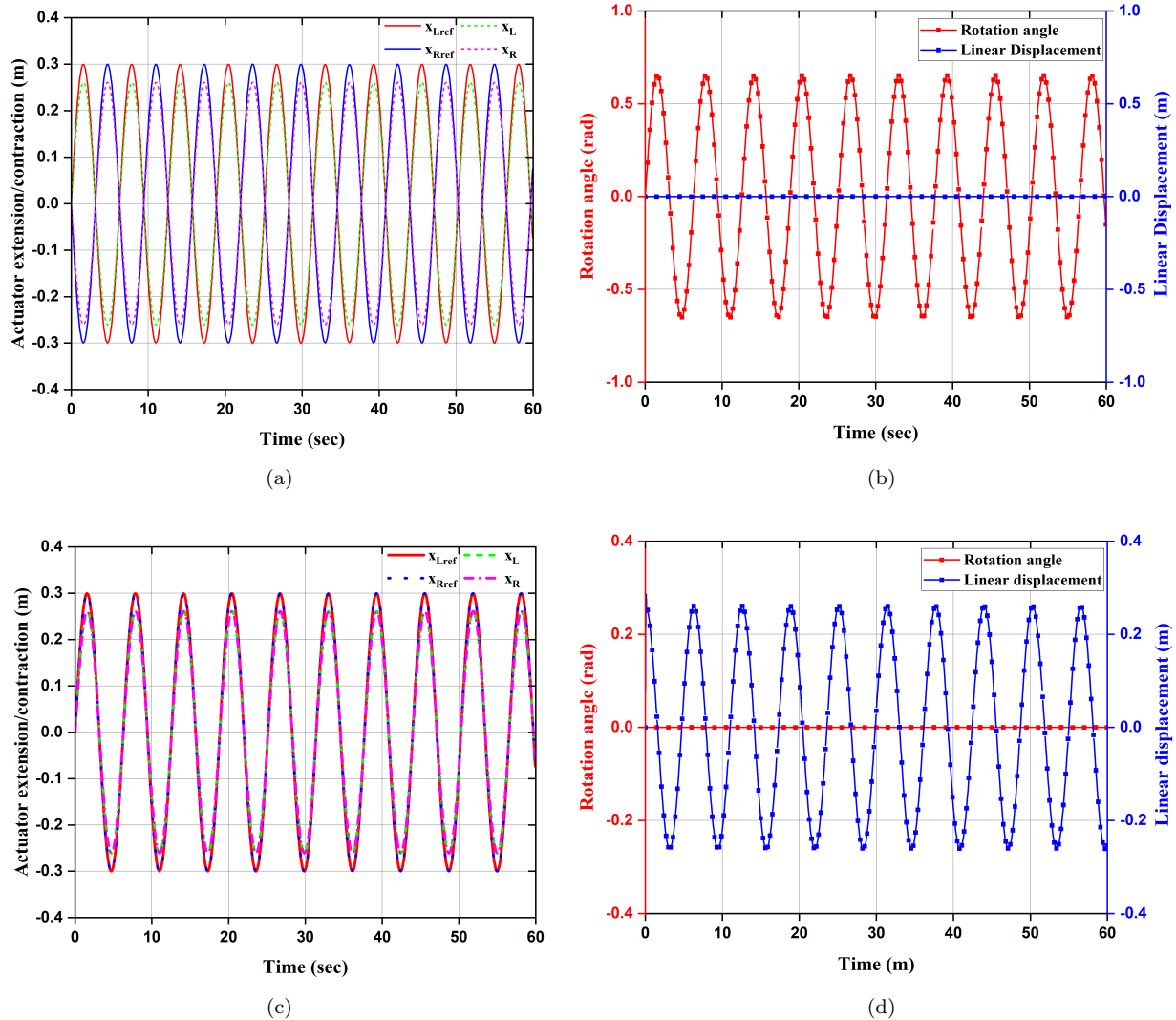


Fig. 5 The behaviour of actuator when (a) air is removed and supplied alternately, (b) rotation and extension due to alternate air supply, (c) air is removed and supplied simultaneously, and (d) rotation and extension due to simultaneous air supply.

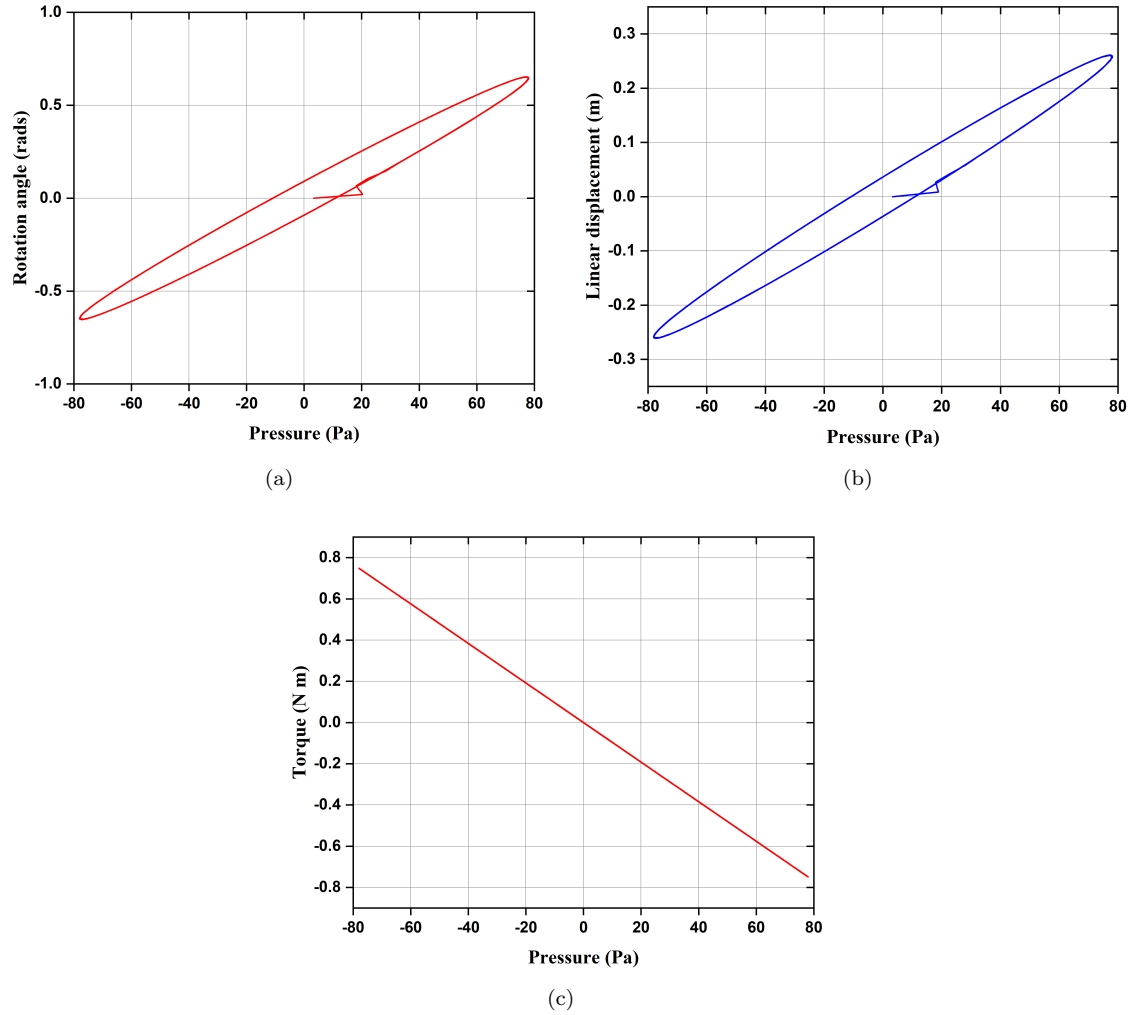


Fig. 6 Performance of actuator in terms of (a) rotation, (b) linear displacement, and (c) torque obtained for the controlled output.

4 Conclusion

The paper presented a design and dynamic modelling of the soft actuator, which can be used in the varied application. The dynamics developed in this paper will be the basis for the complete dynamic modelling of the manipulator or robot created using our actuator. The conventional PD control is used in this paper, but we can use superior control methods since we have an accurate dynamic model. It would be interesting for future studies to achieve other important objectives such as path planning and obstacle avoidance for a soft robot made from the soft actuator.

Acknowledgment

This work was supported in part by Indo-Korea JNC Program of Department of Science and Technology (DST), Government of India (INT/Korea/JNC/Robotics, dated 23-03-2018), in part by the National Research Foundation of Korea (NRF-2017K1A3A1A68072072).

References

- Blumenschein LH, Gan LT, Fan JA, Okamura AM, Hawkes EW (2018) A tip-extending soft robot enables reconfigurable and deployable antennas. *IEEE Robotics and Automation Letters* 3(2):949–956, DOI 10.1109/LRA.2018.2793303
- Bolton W (1999) *Mechatronics: Electronic control systems in mechanical engineering*. Addison Wesley Longman, Harlow, Essex, England
- Boyraz P, Runge G, Raatz A (2018) An overview of novel actuators for soft robotics. *Actuators* 7(3), DOI 10.3390/act7030048, URL <https://www.mdpi.com/2076-0825/7/3/48>
- Chen C, Tang W, Hu Y, Lin Y, Zou J (2020) Fiber-reinforced soft bending actuator control utilizing on/off valves. *IEEE Robotics and Automation Letters* 5(4):6732–6739, DOI 10.1109/LRA.2020.3015189
- Controllab Products (2018) 20sim. URL <https://www.20sim.com>
- Deimel R, Brock O (2013) A compliant hand based on a novel pneumatic actuator. In: 2013 IEEE International Conference on Robotics and Automation, pp 2047–2053, DOI 10.1109/ICRA.2013.6630851
- Deimel R, Radke M, Brock O (2016) Mass control of pneumatic soft continuum actuators with commodity components. In: 2016 IEEE/RSJ International Conference on Intelligent Robots and Systems (IROS), IEEE Press, p 774–779, DOI 10.1109/IROS.2016.7759139, URL <https://doi.org/10.1109/IROS.2016.7759139>
- Elango N, Faudzi AAM (2015) A review article: investigations on soft materials for soft robot manipulations. *The International Journal of Advanced Manufacturing Technology* 80(5):1433–3015, DOI 10.1007/s00170-015-7085-3
- Elango N, Razif MR, Faudzi AAM, Palanikumar K (2020) Evaluation of a suitable material for soft actuator through experiments and fe simulations. *International Journal of Manufacturing, Materials, and Mechanical Engineering* 10(2):64–76, DOI 10.4018/IJMMME.2020040104
- Falkenhahn V, Hildebrandt A, Neumann R, Sawodny O (2017) Dynamic control of the bionic handling assistant. *IEEE/ASME Transactions on Mechatronics* 22(1):6–17, DOI 10.1109/TMECH.2016.2605820
- Gerboni G, Diodato A, Ciuti G, Cianchetti M, Menciassi A (2017) Feedback control of soft robot actuators via commercial flex bend sensors. *IEEE/ASME Transactions on Mechatronics* 22(4):1881–1888, DOI 10.1109/TMECH.2017.2699677
- Greer JD, Morimoto TK, Okamura AM, Hawkes EW (2017) Series pneumatic artificial muscles (spams) and application to a soft continuum robot. In: 2017 IEEE International Conference on Robotics and Automation (ICRA), pp 5503–5510, DOI 10.1109/ICRA.2017.7989648
- Huang H, Lin J, Wu L, Fang B, Sun F (2019) Optimal control scheme for pneumatic soft actuator under comparison of proportional and pwm-solenoid valves. *Photonic Network Communications* 37(2):153–163, DOI 10.1007/s11107-018-0815-3, URL <https://doi.org/10.1007/s11107-018-0815-3>
- Hyatt P, Wingate D, Killpack MD (2019) Model-based control of soft actuators using learned non-linear discrete-time models. *Frontiers in Robotics and AI* 6:22, DOI 10.3389/frobt.2019.00022, URL <https://www.frontiersin.org/article/10.3389/frobt.2019.00022>

- Laschi C, Mazzolai B, Cianchetti M (2016) Soft robotics: Technologies and systems pushing the boundaries of robot abilities. *Science Robotics* 1(1), DOI 10.1126/scirobotics.aah3690
- Li M, Kang R, Branson DT, Dai JS (2018) Model-free control for continuum robots based on an adaptive kalman filter. *IEEE/ASME Transactions on Mechatronics* 23(1):286–297, DOI 10.1109/TMECH.2017.2775663
- Marchese AD, Tedrake R, Rus D (2016) Dynamics and trajectory optimization for a soft spatial fluidic elastomer manipulator. *The International Journal of Robotics Research* 35(8):1000–1019, DOI 10.1177/0278364915587926, URL <https://doi.org/10.1177/0278364915587926>, <https://doi.org/10.1177/0278364915587926>
- Mohd Nordin INA, Muhammad Razif MR, Faudzi AAM, Natarajan E, Iwata K, Suzumori K (2013) 3-d finite-element analysis of fiber-reinforced soft bending actuator for finger flexion. In: 2013 IEEE/ASME International Conference on Advanced Intelligent Mechatronics, pp 128–133, DOI 10.1109/AIM.2013.6584080
- Polygerinos P, Wang Z, Overvelde JTB, Galloway KC, Wood RJ, Bertoldi K, Walsh CJ (2015) Modeling of soft fiber-reinforced bending actuators. *IEEE Transactions on Robotics* 31(3):778–789, DOI 10.1109/TRO.2015.2428504
- Skorina EH, Luo M, Tao W, Chen F, Fu J, Onal CD (2017) Adapting to flexibility: Model reference adaptive control of soft bending actuators. *IEEE Robotics and Automation Letters* 2(2):964–970, DOI 10.1109/LRA.2017.2655572
- Thor Morales B, Frederick L, Alexandre K, Zhongkai Z, Rochdi M, Christian D (2018) Finite element method-based kinematics and closed-loop control of soft, continuum manipulators. *Soft Robotics* 5(3):348–364, DOI 10.1089/soro.2017.0079
- Wu P, Jiangbei W, Yanqiong F (2018) The structure, design, and closed-loop motion control of a differential drive soft robot. *Soft Robotics* 5(1):71–80, DOI 10.1089/soro.2017.0042
- Zhang J, Sheng J, O'Neill CT, Walsh CJ, Wood RJ, Ryu JH, Desai JP, Yip MC (2019) Robotic artificial muscles: Current progress and future perspectives. *IEEE Transactions on Robotics* 35(3):761–781, DOI 10.1109/TRO.2019.2894371

Nomenclature

- μ Transformer coefficient in bond graph model
- ρ Density of air supplied by air pump
- ω Angular frequency for desired extension/contraction
- A Area of elastic packet
- C_d Orifice coefficient of discharge
- D Diameter of orifice in elastic packet for air supply/removal
- k Stiffness of elastic packet
- k_d Derivative gain constant
- k_p Proportional gain constant

- m Mass of elastic packet
- R Gas constant
- R_b Damping in elastic packet
- T Temperature of air supplied
- x Amplitude of desired reference trajectory